Exceptionally bright TeV flares from the binary LS I +61° 303

S. Archambault[1], A. Archer[2], T. Aune[3], A. Barnacka[4], W. Benbow[5], R. Bird[6], V. Bugaev[2], M. Cerruti[5], X. Chen[7,8], L. Ciupik[9], W. Cui[10], J. D. Eisch[11], J. P. Finley[10], H. Fleischhack[8], A. Flinders[12], L. Fortson[13], G. H. Gillanders[14], S. Griffin[1], J. Grube[9], G. Gyuk[9], M. Hütten[8], D. Hanna[1], J. Holder[15], P. Kaaret[16], P. Kar[12], M. Kertzman[17], Y. Khassen[6], D. Kieda[12], M. Krause[8], F. Krennrich[11], M. J. Lang[14], K. Meagher[18], P. Moriarty[14], A. O'Faoláin de Bhróithe[8], R. A. Ong[3], A. N. Otte[18], N. Park[19], M. Pohl[7,8], A. Popkow[3], E. Pueschel[6], J. Quinn[6], K. Ragan[1], G. T. Richards[18], E. Roache[5], G. H. Sembroski[10], A. W. Smith[20], I. Telezhinsky[7,8], J. V. Tucci[10], J. Tyler[1], S. Vincent[8], S. P. Wakely[19], O. M. Weiner[21]

ABSTRACT

The TeV binary system LS I +61° 303 is known for its regular, non-thermal emission pattern which traces the orbital period of the compact object in its 26.5 day orbit around its B0 Ve star companion. The system typically presents elevated TeV emission around apastron passage with flux levels between 5 and 15 % of the steady flux from the Crab Nebula (> 300 GeV). In this article, VERITAS observations of LS I +61° 303 taken in late 2014 are presented, during which bright TeV flares around apastron at flux levels peaking above 30% of the Crab Nebula flux were detected. This is the brightest such activity from this source ever seen in the TeV regime. The strong outbursts have rise and fall times of less than a day. The short timescale of the flares, in conjunction with the observation of 10 TeV photons from LS I +61° 303 during the flares, provides constraints on the nature and efficiency of the accelerating mechanism in the source.

Subject headings: binaries: general — gamma rays: observations — stars: individual (LS I +61° 303) — stars: individual (VER J0240+612)— X-rays: binaries

[1]Physics Department, McGill University, Montreal, QC H3A 2T8, Canada

[2]Department of Physics, Washington University, St. Louis, MO 63130, USA

[3]Department of Physics and Astronomy, University of California, Los Angeles, CA 90095, USA

[4]Harvard-Smithsonian Center for Astrophysics, 60 Garden Street, Cambridge, MA 02138, USA

[5]Fred Lawrence Whipple Observatory, Harvard-Smithsonian Center for Astrophysics, Amado, AZ 85645, USA

[6]School of Physics, University College Dublin, Belfield, Dublin 4, Ireland

[7]Institute of Physics and Astronomy, University of Potsdam, 14476 Potsdam-Golm, Germany

[8]DESY, Platanenallee 6, 15738 Zeuthen, Germany

[9]Astronomy Department, Adler Planetarium and Astronomy Museum, Chicago, IL 60605, USA

[10]Department of Physics and Astronomy, Purdue University, West Lafayette, IN 47907, USA

[11]Department of Physics and Astronomy, Iowa State University, Ames, IA 50011, USA

[12]Department of Physics and Astronomy, University of Utah, Salt Lake City, UT 84112, USA

[13]School of Physics and Astronomy, University of Minnesota, Minneapolis, MN 55455, USA

[14]School of Physics, National University of Ireland Galway, University Road, Galway, Ireland

[15]Department of Physics and Astronomy and the Bartol Research Institute, University of Delaware, Newark, DE 19716, USA

[16]Department of Physics and Astronomy, University of Iowa, Van Allen Hall, Iowa City, IA 52242, USA

[17]Department of Physics and Astronomy, DePauw University, Greencastle, IN 46135-0037, USA

[18]School of Physics and Center for Relativistic Astrophysics, Georgia Institute of Technology, 837 State Street NW, Atlanta, GA 30332-0430

[19]Enrico Fermi Institute, University of Chicago, Chicago,

1. Introduction

High-mass X-ray binaries (HMXBs) are a class of binary system that consist of a compact object (either a black hole or a neutron star) and a massive stellar companion, and emit in X-rays. The current generation of imaging atmospheric-Cherenkov telescopes (IACTs) has facilitated the study of HMXBs which exhibit TeV emission. The class of TeV binaries is quite sparse, consisting of only a handful of sources: LS 5039 (Aharonian et al. 2005b), PSR B1259-63 (Aharonian et al. 2005a), LS I +61° 303 (Albert et al. 2006), HESS J0632+057 (Aharonian et al. 2007), 1FGL J1018.6-5856 (Abramowski et al. 2015), and the newest member of the class, TeV 2032+413 (Lyne et al. 2015). Of these, only the compact objects of PSR B1259-63 and TeV 2032+413 have been firmly identified as pulsars. There is still a large degree of ambiguity concerning the nature of the compact object within the other systems. Consequently, the fundamental mechanism responsible for the TeV emission along with its characteristic variability on the timescale of one orbital period remains uncertain.

The orbital periods of TeV-emitting HMXBs vary from several days (LS 5039) to many years (TeV 2032+413). As the TeV emission varies strongly as a function of the orbital phase, the various sources may only have short windows during which they can be detected and studied in the TeV regime. Of the TeV binaries, LS I +61° 303 is the only known source in the Northern Hemisphere that has a short enough orbital period (26.5 days) to allow for regular study with TeV instruments.

Located at a distance of $\sim$ 2 kpc (Frail & Hjellming 1991), LS I +61° 303 is composed of a B0 Ve star and a compact object (Hutchings & Crampton 1981; Casares et al. 2005). The observed multiwavelength emission is variable at all energies and modulated with a period of $P \approx 26.5$ days, believed to be associated with the orbital motion of the binary system (Taylor & Gregory 1982; Paredes et al. 1994, 1997; Esposito et al. 2007; Abdo et al. 2009; Albert et al. 2006; Acciari et al. 2008). Radial velocity measurements show the orbit to be elliptical with eccentricity $e = 0.537 \pm 0.034$, with periastron occurring around phase $\phi = 0.275$, apastron at $\phi = 0.775$, superior conjunction at $\phi = 0.081$ and inferior conjunction at $\phi = 0.313$ (Aragona et al. 2009). The periastron distance between the star and the compact object is estimated at 2.84×10^{12} cm (0.19 AU) and the apastron distance at 9.57×10^{12} cm (0.64 AU) (Dubus 2013). However, the inclination of the system is not exactly known but is expected to lie in the range 10° – 60° according to Casares et al. (2005), leading to some uncertainty in the orbital parameters.

In this work, we present the results of the VERITAS campaign on LS I +61° 303 in October – December of 2014. During this time, VERITAS observed historically bright flares from LS I +61° 303 around apastron, with the source exhibiting flux levels a factor of 2 – 3 times higher than ever observed.

2. Observations

The VERITAS IACT array, located at the base of Mt. Hopkins, Arizona (1.3 km a.s.l., 31°40′ N, 110°57′ W) consists of four 12 m diameter Davies-Cotton design optical telescopes. VERITAS is sensitive to photons with energies from 85 GeV to 30 TeV and has the ability to detect a 1 % Crab Nebula source in approximately 25 hours[1]. For a full description of the hardware components and analysis methods utilized by VERITAS, see Holder et al. (2008); Kieda, D. (2013); Acciari et al. (2008), and references therein.

In the 2014 season, VERITAS observations of LS I +61° 303 were taken from October 16 (MJD 56946) to December 12 (MJD 57003), comprising a total of 23.3 hours of quality-selected live-time. These observations sampled three separate orbital periods, covering the orbital phase regions of $\phi = 0.5 - 0.2$ (see Figure 1 and Table 1). Over the entire set of observations, a total of 443 excess events ($N_{\rm on} = 705$, $N_{\rm off} = 2883$, $\alpha = 0.0909$) above an energy threshold of 300 GeV were detected above background. This is equivalent to a statistical significance of 21 standard deviations (21σ, calculated using Equation 17 of Li & Ma

IL 60637, USA

[20]University of Maryland, College Park / NASA GSFC, College Park, MD 20742, USA

[21]Physics Department, Columbia University, New York, NY 10027, USA

[1]http://veritas.sao.arizona.edu/specifications

1983).

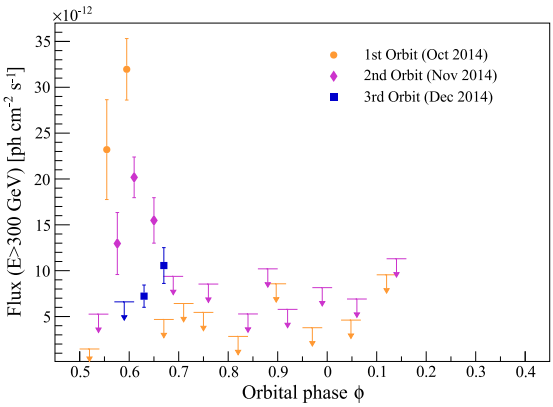

Fig. 1.— Light curve of LS I +61° 303 during the 2014 observation season shown as a function of orbital phase in nightly bins. The phase range is shown from 0.45 – 0.45 as the VERITAS observations commenced around a phase of $\phi = 0.5$ in each orbit. The data for the first orbit (October) are shown with orange circles, while the second orbit (November) is represented by purple diamonds, and the third (December) by blue squares. Flux upper limits at the 99% confidence level (using the unbounded approach of Rolke et al. 2005) are shown for points with significance $< 3\,\sigma$ and are represented by arrows.

During the first orbit observed (in October), the source presented the largest of its flares (hereafter "F1"), beginning on 2014 October 17 (MJD 56947, $\phi = 0.55$). The emission reached a peak flux of $(3.20 \pm 0.34) \times 10^{-11}$ cm^{-2} s^{-1} above 300 GeV on October 18 (MJD 56948, $\phi = 0.60$). This flare reached a peak flux of approximately 30% of the Crab Nebula flux above the same energy threshold, representing the largest flux ever detected from the source. Unfortunately, observations were limited by poor weather conditions the following two nights and only recommenced on October 20 (MJD 56950), by which time the flux from the source had already decreased. During the second orbital passage in November, VERITAS detected another period of elevated flux ("F2") from the source at similar orbital phases ($\phi = 0.55 - 0.65$) with peak emission of $(2.02 \pm 0.22) \times 10^{-11}$ cm^{-2} s^{-1} on November 14 (MJD 56975, $\phi = 0.61$).

As an initial test to show that the TeV flux is not stable, the light curves of each orbit were fitted with a constant flux model. Both F1 and F2 were found to be inconsistent with this model at the $10\,\sigma$ level. A test for variability on a nightly timescale was then performed over the complete time range of these observations. For each pair of nightly separated fluxes (F_1, F_2) with statistical errors (σ_1, σ_2), the absolute value of the difference of the fluxes was calculated and the errors propagated using the usual variance formula. The probability that the two fluxes are not the same (i.e., $F_1 \neq F_2$) was found in terms of the standard deviation by dividing the difference by the error:

$$S(F_1 \neq F_2) = \frac{|F_1 - F_2|}{\sqrt{(\sigma_1^2 + \sigma_2^2)}}. \quad (1)$$

The most significant difference was found between the first and second nights of F1, with a pre-trials significance of $5.15\,\sigma$ corresponding to a post-trials significance of $4.66\,\sigma$ when accounting for the 12 pairs of nightly separated observations. Overall, the data are too sparsely sampled to allow a good measure the rise and fall times of the flares. However, the strong statistical indication of nightly variability and the sharp transition from a flux upper limit to a significantly detected flux over the course of 24 hours at the onset of F1 and F2 imply that the rise time of the flares is of the order of less than one day.

Follow-up observations conducted by VERITAS during the next month (December) covered the orbital phases of $\phi = 0.59 - 0.67$ and detected the source at a lower flux level. The previous flares in 2014 were detected at $\phi \simeq 0.60$, but during this cycle the source reached only $(0.72 \pm 0.12) \times 10^{-11}$ cm^{-2} s^{-1} at a comparable orbital phase on December 11 (MJD 57002, $\phi = 0.63$). The peak emission of this cycle occurred on the following night at an orbital phase of $\phi = 0.67$. The light curve of this orbit was also fitted with a constant flux model and was found to be consistent within $\sim 3\,\sigma$. The observations during this month seem to exclude the type of peaked flaring behavior seen around the orbital phase $\phi \simeq 0.60$ in the previous two orbital cycles, indicating some orbit-to-orbit variations in the source.

The average differential photon spectrum from all observations of LS I +61° 303 during the 2014 observing season is well fit with a power law of the

TABLE 1

VERITAS OBSERVATIONS OF LS I +61° 303 IN 2014. THE ERRORS QUOTED ON THE FLUX ARE STATISTICAL ONLY. THE LAST COLUMN SHOWS THE PRE-TRIALS SIGNIFICANCE OF THE FLUX DIFFERENCE FOR EACH PAIR OF NIGHTLY SEPARATED FLUXES IN UNITS OF STANDARD DEVIATION. THE SECTIONS SHOW THE DIVISION OF THE DATA ACROSS THE THREE SETS OF OBSERVATIONS TAKEN IN OCTOBER, NOVEMBER, AND DECEMBER, RESPECTIVELY.

Date [MJD]	Orbital phase, ϕ	Flux(>300 GeV) [$\times 10^{-11}$ cm^{-2} s^{-1}]	Duration [mins]	S($F_1 \neq F_2$) [σ]
56946.3	0.52	<0.15	24.5	–
56947.3	0.55	2.32 ± 0.54	21.0	5.15
56948.3	0.60	3.20 ± 0.34	74.5	1.38
56950.0	0.67	<0.47	51.5	–
56951.0	0.71	<0.64	51.1	0.94
56952.0	0.75	<0.55	51.0	0.56
56954.0	0.82	<0.28	51.1	–
56956.0	0.90	<0.86	51.5	–
56958.0	0.97	<0.38	50.3	–
56960.0	0.05	<0.46	50.7	–
56962.0	0.12	<0.96	50.7	–
56973.0	0.54	<0.53	25.5	–
56974.0	0.58	1.30 ± 0.34	34.4	3.63
56975.0	0.61	2.02 ± 0.22	111.3	1.80
56976.0	0.65	1.55 ± 0.25	65.4	1.42
56977.0	0.69	<0.94	54.5	3.74
56979.0	0.76	<0.85	25.7	–
56981.0	0.84	<0.53	51.3	–
56982.0	0.88	<1.02	25.7	0.57
56983.0	0.92	<0.58	33.4	0.62
56985.0	0.99	<0.82	48.8	–
56987.0	0.06	<0.69	51.9	–
56989.0	0.14	<1.13	51.6	–
57001.0	0.59	<0.66	64.6	–
57002.0	0.63	0.72 ± 0.12	144.3	2.67
57003.0	0.67	1.06 ± 0.20	80.2	1.48

form

$$\frac{dN}{dE} = N_0 \left(\frac{E}{1\,\mathrm{TeV}} \right)^{-\Gamma}, \qquad (2)$$

in which N_0 is the normalization at the pivot energy of 1 TeV, and Γ is the spectral index. The measured parameters are consistent with past observations. Differential photon spectra were also extracted from F1 (October 17 – 18) and F2 (November 13 – 15) and show a similar spectral shape, albeit with a higher normalization constant. No spectral variability is detected within the statistical errors. The parameters from the spectral fits are given in Table 2. An uncertainty on the energy scale of 15 – 25% results in a systematic uncertainty of $\sim 20\%$ on the flux normalization and $\sim 40\%$ on the integral flux, assuming a spectral index of 2.34. The systematic uncertainty on the spectral index is estimated at ~ 0.3, accounting for uncertainties on the collection efficiency, sky brightness, analysis cuts and simulation model. All spectra are shown in Figure 2 along with previous spectral measurements (Acciari et al. 2008; Aleksić et al. 2012) for comparison.

The highest energy gamma-ray candidates observed were detected during the peak night of F1 with an energy of ~ 10 TeV. There are no events in the OFF region with energies above 4 TeV on this night, so it is assumed that the contribution of the background at ~ 10 TeV is negligible.

During these observations, the source was also monitored by the *Fermi*-LAT (0.1 – 300 GeV), the *Swift*-XRT (0.2 – 10 keV), and both the RATAN and AMI radio instruments (4/6 – 15 GHz). In addition, Hα monitoring of the system took place at the Ritter Observatory in Toledo, Ohio (USA). After F2 was detected by VERITAS, an Astronomer's Telegram[2] (Holder 2015) was released, notifying the astronomical community of the historic flux levels and triggering more intense observations by multiwavelength partners, as well as additional observations with the MAGIC TeV observatory. The results of this multiwavelength campaign are under analysis and will be presented in a future publication.

[2] www.astronomerstelegram.org

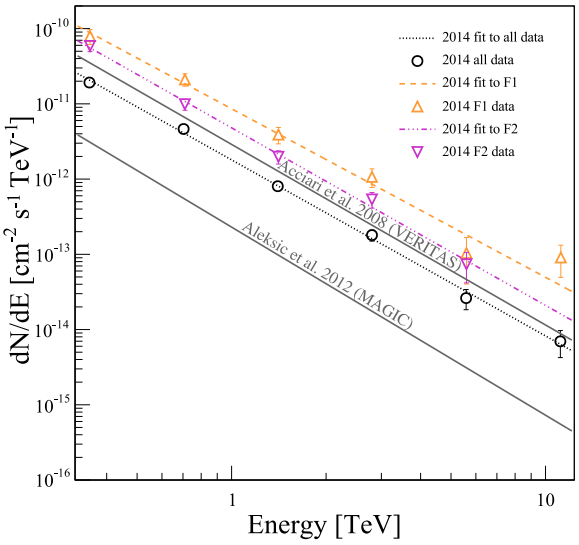

Fig. 2.— Average and flare differential photon spectra of LS I +61° 303 from the VERITAS 2014 observations, shown in comparison with the average spectra from Acciari et al. (2008) and Aleksić et al. (2012).

3. Discussion and Conclusion

The nature of the compact object in LS I +61° 303 is not firmly established and, as a result, proposed emission mechanisms for the system cover a range of possibilities. These mechanisms fall into two main categories: microquasar (μQ) and pulsar binary (PB). In the μQ scenario, non-thermal particle-acceleration processes occur in the jet of an accreting compact object (Massi et al. 2001; Massi & Jaron 2013; Massi et al. 2015), whereas the binary pulsar scenario utilizes the presence of a shocked wind in which particle acceleration is the result of the interaction between the stellar and the pulsar winds (Dhawan et al. 2006). While some versions of both models utilize a hadronic primary population, the majority of both model types employ leptonic origins for the observed non-thermal emission. In a leptonic scenario, the TeV emission is the result of inverse-Compton (IC) scattering of electrons accelerated in the jet (μQ) or at the shock front (PB).

Paredes-Fortuny et al. (2015) present a general pulsar wind shock scenario with an inhomogeneous

TABLE 2

SPECTRAL PARAMETERS OF THE POWER LAW FITS TO THE OBSERVATIONS OF LS I +61° 303 IN THE ENERGY RANGE 0.3 – 20 TEV.

Observations	Normalization [$\times 10^{-12}$ cm^{-2} s^{-1} TeV^{-1}]	Spectral index
All (average)	$1.8 \pm 0.1_{\rm stat} \pm 0.4_{\rm sys}$	$2.34 \pm 0.07_{\rm stat} \pm 0.3_{\rm sys}$
F1 (Oct 17 – 18)	$8.6 \pm 1.0_{\rm stat} \pm 1.7_{\rm sys}$	$2.24 \pm 0.12_{\rm stat} \pm 0.3_{\rm sys}$
F2 (Nov 13 – 15)	$4.8 \pm 0.4_{\rm stat} \pm 1.0_{\rm sys}$	$2.36 \pm 0.12_{\rm stat} \pm 0.3_{\rm sys}$

stellar wind in which the B0 Ve star disc is disrupted and fragments. The resulting clumps of the disc fall into the shock region, pushing the shock closer to the pulsar. The reduction in size of the pulsar wind termination shock could allow for increased acceleration efficiency on the timescale of a few hours, depending on the size and density of the disc fragments. Such a scenario could account for the exceptionally bright TeV flares and orbit-to-orbit variations seen in LS I +61° 303.

Regardless of the primary mechanism of generation, Khangulyan et al. (2008) provide a prescription to calculate model-independent limits on the magnetic field strength and the efficiency of the accelerator within an IC scenario. Given the temperature $T = 2.25 \times 10^4$ K (Dubus 2013) of the B0 Ve star in LS I +61° 303, the average energy of the stellar photons is $3kT \approx 6$ eV, and the IC scattering will take place deep in the Klein-Nishina regime, in which almost all of the electron energy is transferred to the scattered photons. Thus, the presence of ~ 10 TeV photons requires electrons with an energy of at least 10 TeV in the emitter, as well as forcing the acceleration time to be less than the cooling time. As the photon will not carry all the energy from the electron and there is no evidence of a cutoff in the photon spectrum, an example case of a 20 TeV electron will be used in this discussion. Following the calculations of Khangulyan et al. (2008), the acceleration timescale of the electrons can be expressed as

$$t_{\rm acc} = \eta_{\rm acc} r_{\rm L} c^{-1} \approx 0.1 \eta_{\rm acc} \left(\frac{E}{1\,{\rm TeV}}\right) \left(\frac{B}{1\,{\rm G}}\right)^{-1} {\rm s}, \quad (3)$$

where $r_{\rm L}$ is the Larmor radius of the electron, $\left(\frac{E}{1\,{\rm TeV}}\right)$ is the energy of the electron in units of TeV, $\left(\frac{B}{1\,{\rm G}}\right)$ is the magnetic field strength in units of Gauss, and $\eta_{\rm acc} > 1$ is a parameter describing the efficiency of the accelerator (in general $\eta_{\rm acc} \gg 1$). The characteristic cooling time of electrons in the Klein-Nishina regime is given by

$$t_{\rm KN} \approx 10^3 \left(\frac{d}{10^{13}\,{\rm cm}}\right)^2 \left(\frac{E}{1\,{\rm TeV}}\right)^{0.7} {\rm s}, \quad (4)$$

where $\left(\frac{d}{10^{13}\,{\rm cm}}\right)$ is the distance between the emitter and the optical star in units of 10^{13} cm, and the synchrotron cooling time is

$$t_{\rm sy} \approx 4 \times 10^2 \left(\frac{B}{1\,{\rm G}}\right)^{-2} \left(\frac{E}{1\,{\rm TeV}}\right)^{-1} {\rm s}. \quad (5)$$

The relation $t_{\rm KN} < t_{\rm sy}$ can also be set due to the fact that IC losses in the Klein-Nishina regime allow for the hard electron spectra (harder than 2) necessary to produce hard gamma-ray spectral indices (from 2 to 2.5). Thus, the magnetic field in the emitter is constrained by the relation

$$B < 0.6 \left(\frac{d}{10^{13}\,{\rm cm}}\right)^{-1} \left(\frac{E}{1\,{\rm TeV}}\right)^{-0.85} {\rm G}. \quad (6)$$

Using $\left(\frac{E}{1\,{\rm TeV}}\right) = 20$ gives a value of $B \lesssim 0.05$ G at apastron (close to the position in the orbit at which the flares were detected), assuming that the emitter is located close to the compact object.

A fundamental condition is that the Larmor radius of the electrons must be less than the linear size of the emitter. The distance between the optical star and the location of the emitter can be taken as an upper limit on the extent of the emitting region. As before, it is assumed that the emitter is located close to the compact object, so the distance between the compact object and the emitter is used as an estimate of the linear size of the emitter. Rearranging Equation 3 and including this condition on $r_{\rm L}$ yields

$$B > 3 \times 10^{-3} \left(\frac{E}{1\,{\rm TeV}}\right) \left(\frac{d}{10^{12}\,{\rm cm}}\right)^{-1}. \quad (7)$$

This gives a value of $B \gtrsim 6 \times 10^{-3}$ G at apastron.

As the cooling time is dominated by $t_{\rm KN}$, the requirement that the acceleration time is less than the cooling time yields the relation $t_{\rm acc} < t_{\rm KN}$ which gives

$$B > 10^{-4} \left(\frac{d}{10^{13}\,{\rm cm}}\right)^{-2} \left(\frac{E}{1\,{\rm TeV}}\right)^{0.3} \eta_{\rm acc}\ {\rm G}. \quad (8)$$

This expression can be used in conjunction with the lower limit on the magnetic field strength from Equation 7 in order to place a limit on the acceleration efficiency parameter of $\eta_{\rm acc} \lesssim 22$. This value indicates that the emitter must be host to an extremely efficient acceleration process.

The constraints are strongly dependent on the assumed location of the emitter, which has been taken to be coincident with the compact object in order to derive these limits. If the emitter is located further from the star, the limit on the acceleration efficiency parameter is less constraining, but the upper limit on the magnetic field is reduced. Regardless of the location of the emitter, the simple Klein-Nishina scattering assumed in this discussion implies a very hard synchrotron spectrum in the X-ray band. Photon indices softer than 1.3 in this energy regime (Kar 2015) may challenge this simple scenario, which requires an electron spectral index harder than 2 to produce hard gamma-ray spectral indices.

The VERITAS observations of the bright flares from LS I +61° 303 in 2014 provide constraints on the physical properties of the system around the acceleration region as well as on the efficiency of the acceleration mechanism. However, these constraints are not enough to hint at either a μQ or PB system. While the detection of pulsed emission from the source would unambiguously identify the compact object as a pulsar, it is also possible that the dense stellar environment of the source could hinder such a detection. Regardless, further observations of LS I +61° 303 with TeV instruments are necessary to fully understand the varying TeV emission from this source.

This research is supported by grants from the U.S. Department of Energy Office of Science, the U.S. National Science Foundation and the Smithsonian Institution, and by NSERC in Canada. We acknowledge the excellent work of the technical support staff at the Fred Lawrence Whipple Observatory and at the collaborating institutions in the construction and operation of the instrument. The VERITAS Collaboration is grateful to Trevor Weekes for his seminal contributions and leadership in the field of VHE gamma-ray astrophysics, which made this study possible. A. O'FdB acknowledges support through the Young Investigators Program of the Helmholtz Association. A.W. Smith acknowledges support from the Fermi Cycle 7 Guest Investigator Program, grant number NNH13ZDA001N.

REFERENCES

Abdo, A. A., Ackermann, M., Ajello, M., et al. 2009, ApJ, 701, L123

Abramowski, A., Aharonian, F., Ait Benkhali, F., et al. 2015, A&A, 577, A131

Acciari, V. A., Beilicke, M., Blaylock, G., et al. 2008, ApJ, 679, 1427

Aharonian, F., Akhperjanian, A. G., Aye, K.-M., et al. 2005a, A&A, 442, 1

—. 2005b, Science, 309, 746

Aharonian, F. A., Akhperjanian, A. G., Bazer-Bachi, A. R., et al. 2007, A&A, 469, L1

Albert, J., Aliu, E., Anderhub, H., et al. 2006, Science, 312, 1771

Aleksić, J., Alvarez, E. A., Antonelli, L. A., et al. 2012, ApJ, 746, 80

Aragona, C., McSwain, M. V., Grundstrom, E. D., et al. 2009, ApJ, 698, 514

Casares, J., Ribas, I., Paredes, J. M., Martí, J., & Allende Prieto, C. 2005, MNRAS, 360, 1105

Dhawan, V., Mioduszewski, A., & Rupen, M. 2006, in Proc. of Microquasars and Beyond: From Binaries to Galaxies, in Proceedings of Science, Como, Italy, ed. T. Belloni, p.52

Dubus, G. 2013, A&A Rev., 21, 64

Esposito, P., Caraveo, P. A., Pellizzoni, A., et al. 2007, A&A, 474, 575

Frail, D. A., & Hjellming, R. M. 1991, AJ, 101, 2126

Holder, J. 2015, The Astronomer's Telegram, 6785

Holder, J., Acciari, V. A., Aliu, E., et al. 2008, American Institute of Physics Conference Series, 1085, 657

Hutchings, J., & Crampton, D. 1981, PASP, 93, 486

Kar, P. 2015, ArXiv e-prints, arXiv:1508.06674

Khangulyan, D., Aharonian, F., & Bosch-Ramon, V. 2008, MNRAS, 383, 467

Kieda, D. 2013, in Proceedings of the 33rd International Cosmic Ray Conference (ICRC2013)

Li, T.-P., & Ma, Y.-Q. 1983, The Astrophysical Journal, 272, 317

Lyne, A. G., Stappers, B. W., Keith, M. J., et al. 2015, MNRAS, 451, 581

Massi, M., & Jaron, F. 2013, A&A, 554, A105

Massi, M., Jaron, F., & Hovatta, T. 2015, A&A, 575, L9

Massi, M., Ribó, M., Paredes, J. M., Peracaula, M., & Estalella, R. 2001, A&A, 376, 217

Paredes, J. M., Marti, J., Peracaula, M., & Ribo, M. 1997, A&A, 320, L25

Paredes, J. M., Marziani, P., Marti, J., et al. 1994, A&A, 288, 519

Paredes-Fortuny, X., Bosch-Ramon, V., Perucho, M., & Ribó, M. 2015, A&A, 574, A77

Rolke, W. A., López, A. M., & Conrad, J. 2005, Nuclear Instruments and Methods in Physics Research A, 551, 493

Taylor, A. R., & Gregory, P. C. 1982, ApJ, 255, 210

This 2-column preprint was prepared with the AAS LaTeX macros v5.2.